Robotic Endoscope System for Future Application in Minimally Invasive Laser Osteotomy: First Concept Evaluation

Manuela Eugster, Cédric Duverney, Murali Karnam, *Student Member, IEEE*, Nicolas Gerig, Philippe C. Cattin, *Member, IEEE*, and Georg Rauter, *Member, IEEE*

***Abstract*—We are developing a robotic system for future application in minimally invasive laser osteotomy. This paper presents the mechanical system concept as a macro-milli-micro system and focuses on designing and evaluating the milli-system. The milli-system consists of an articulated tendon-driven robotic endoscope with seven rigid links with an outer diameter of 8 mm connected by six discrete rotational joints (±30°). These joints can be controlled individually, however, controlling one joint's motion influences all joints located more distally, making joint control an interesting challenge. Controlling each joint as desired will allow positioning the micro-system mounted at the endoscope's tip. The micro-system is itself a robot that will accurately position the laser. The robotic endoscope incorporates a hollow core with a diameter of 4.8 mm that holds a supply channel for the micro-system with the necessary means for actuation and surgical intervention. We demonstrated the functionality of the robotic endoscope in tracking experiments. Despite the joints' mutual influence, the articulated robotic endoscope could be handled successfully and achieved an angular settling error of less than 1° in the individual joints. The overall robotic system's functionality was successfully demonstrated with a time-synchronized joint movement of the macro-system (serial manipulator) and the robotic endoscope.**

***Index Terms*—Articulated endoscope, tendon-driven robot, actuation unit, minimally invasive surgery, unicondylar knee arthroplasty.**

I. Introduction

LASER osteotomy is a novel alternative for cutting hard tissue such as bone. Compared to conventional machining of bone using mills, drills, and saws, laser osteotomy has promising benefits such as faster healing or increased freedom in the cutting geometry [1]. To enable accurate and, in particular, deep bone cuts, the laser must be moved several times in submillimeter steps along the cutting path. Thus, manual control of a laser osteotome is difficult for surgeons to realize with the required accuracy [2], [3]. Robot-assisted systems have been proposed to help the surgeon accurately guide a laser for bone cutting (e.g., the prototype system based on a CO_2 slab laser, guided by an industrial robot developed by Burgner *et al.* [4]). Since 2021, the first and so far only commercially available robotic laser osteotome is CARLO (Advanced Osteotomy Tools - AOT AG, Basel, Switzerland) [5]. The device is based on a large serial robotic arm that guides the laser. The laser source and optic components are mounted on the end effector of this serial robot. With the approaches for robotic laser osteotomy that exist today [4], [5], direct access (line of sight) to the bone is necessary. Thus, the entire bone that has to be treated must be exposed in open surgery.

Accordingly, less invasive approaches for cutting bone are desirable. Devices for less invasive interventions already exist for other laser applications, such as soft tissue ablation (e.g., for head and neck surgery [6], [7]), or optical biopsies (e.g., confocal microlaparoscopy [8]). In these devices, the laser is placed outside the patient and guided from its source to the surface that is to be treated using a flexible optical fiber. This optical fiber is integrated into a flexible surgical instrument, such as an endoscope. The flexible instrument can reach surgical sites inside the body while adapting to the patient's anatomy. Thus, the procedure can be performed through smaller incisions, and damage to surrounding tissue can be minimized. The laser beam leaves the optical fiber at the flexible instrument's tip, i.e., the last segment of the flexible instrument. In most cases, the laser beam is aligned parallel to the longitudinal axis of the last segment of the flexible instrument.

To our best knowledge, no flexible instrument for minimally invasive bone-cutting applications existed. Also, even the existing flexible instruments for minimally invasive soft tissue treatment are not suitable for performing bone cuts in a minimally invasive procedure. One reason being that these existing flexible instruments require a larger manipulation space above the target surface (usually over 23 mm based on their diameter or length and working distance [9]). This amount of manipulation space is not available during minimally invasive procedures on

Manuscript received 14 March 2021; revised 26 October 2021 and 14 February 2022; accepted 27 April 2022. Date of publication 4 May 2022; date of current version 17 August 2022. This article was recommended for publication by Associate Editor M. Zenati and Editor P. Dario upon evaluation of the reviewers' comments. This work was supported by the Werner Siemens Foundation through the MIRACLE Project. *(Corresponding author: Manuela Eugster.)*

Manuela Eugster, Cédric Duverney, Murali Karnam, Nicolas Gerig, and Georg Rauter are with the BIROMED-Lab, Department of Biomedical Engineering, University of Basel, 4123 Allschwil, Switzerland (e-mail: manuela.eugster@unibas.ch).

Philippe C. Cattin is with the CIAN, Department of Biomedical Engineering, University of Basel, 4123 Allschwil, Switzerland.

This article has supplementary downloadable material available at https://doi.org/10.1109/TMRB.2022.3172471, provided by the authors.

Digital Object Identifier 10.1109/TMRB.2022.3172471

bones such as in joints (maximally 8 mm based on our evaluation [10]).

To enable laser osteotomy also in confined spaces and to facilitate a tissue-sparing treatment option for minimally invasive laser osteotomy in general, we propose a new approach. For delivering the laser light to the target tissue minimally invasively for bone cutting, we decided to guide the optical fiber through a flexible endoscope with a laser positioning device integrated into the endoscope's tip that requires minimal manipulation space above the bone.

As a first benchmark application, we planned to realize bone incisions in the knee to facilitate unicondylar knee replacement. The so-called unicondlyar knee arthroplasty (UKA) is a treatment option for osteoarthritis. Osteoarthritis has a high socio-economic impact, causes severe long-term pain, and is globally the most common cause for physical disability [11], [12]. UKA is a less invasive option for a knee replacement compared to total knee arthroplasty (TKA) and can be chosen when only one knee compartment is affected by osteoarthritis. The advantages of UKA compared to TKA include reduced blood loss [13], lower infection rate [14], less postoperative pain [15], faster recovery [13], better preservation of range-of-motion [16], better function [17], and lower cost [18]. However, UKA is less resistant to component malalignment [19] as compared to TKA. Correct alignment of the implant components is crucial for long-term survival of a unicondylar knee implant [20], since poor implant positioning may lead to early implant wear [21], poor functional results [22], and a higher revision rate [23]. Our device could help to improve UKA in different ways: Accuracy of placement and fixation of implants could be improved by the possibility of functional cutting geometries, such as a dovetail guide. Also, the intervention would become less invasive due to the smaller opening required for inserting the flexible device and the reduced collateral mechanical and thermal tissue damage of laser bone cuts compared to bone-saw cuts [24].

Our final goal was to develop an approach for minimally invasive bone cutting using a robotic endoscope. Focus was on the robotic challenges in realizing a minimally invasive laser osteotome. Work on the challenges in the field of laser physics are presented elsewhere (e.g., high power laser coupling efficiency into optical fibers [25], [26], or real-time tissue differentiation [27]).

In previous work, we presented and evaluated a miniature parallel robot that can accurately position a laser at the intervention site [28]. This laser positioning device is designed to require minimal manipulation space above the bone and can be operated in confined spaces such as inside a joint. We have also investigated cadaveric knee joints to quantify the available manipulation space for robotic instruments during a minimally invasive UKA procedure [10]. However, we did not yet show how this laser positioning device and the supplies required for intervention (e.g., the laser fiber) can be inserted into the patient and deployed at the intervention site in a minimally invasive manner.

Thus, this work focuses on the concept development and the first mechanical implementation of a) an overall system overview designed to allow future minimally invasive insertion of a laser positioning device supplied with an optical fiber, and b) the system component that will be inserted into the patient's body, i.e., a robotic endoscope including a supply channel holding an optical fiber. The presented robotic endoscope has an articulated tendon-driven structure based on rigid links connected by discrete, individually controllable rotational joints. Due to the serial structure and the tendon actuation, the distal joints are influenced by the proximal joints' motion. This mutual influence of the joints is a challenge, and we are determining whether it is possible to control the robotic endoscope with sufficient accuracy. We present working prototypes and a first evaluation of the robotic endoscope and supply channel's tracking accuracy, and test the overall robotic system's basic functionality on a test bench.

II. Methods

We see the main challenge in developing robotic systems for minimally invasive surgery as an interplay of the following requirements:

i) The device should have a large workspace to allow different mounting positions in the operating room while still reaching all necessary surgical sites on the patient.
ii) The device should carry the surgical instrument's weight and corresponding system peripheries such as motors and sensors.
iii) The interaction with the device should be safe and intuitive for the operating room personnel.
iv) The surgical instrument inserted into the patient's body should be small in diameter and dexterous to allow a minimally invasive insertion.
v) The inserted instrument's diameter must be large enough to bring the required tools and supplies to the intervention site.
vi) The surgical instrument must be sufficiently accurate to deploy the instrument tip at the intervention site.
vii) The instrument tip should allow operation in narrow and confined spaces to minimize the intervention's invasiveness.
viii) The instrument tip must perform the desired procedure (i.e., positioning the laser).
ix) The positioning accuracy of the instrument tip should be in accordance with the surgical intervention.

Realizing a robotic system that allows for minimally invasive insertion of a small end-effector with high tip accuracy in a large workspace is a challenge. Applying the macro-milli-micro approach allows to decouple these demanding requirements by designing different subsystems in series: a macro-, a milli-, and a micro-system, each fulfilling parts of the requirements (Fig. 1): The macro-system has a large workspace, is able to carry high loads, e.g., peripheral components for actuation and control of the milli- and micro-system, and is intuitive and safe to use. The milli-system has a smaller diameter, is sufficiently dexterous for minimally invasive insertion, accurate enough to deploy the instrument tip at the target location of intervention, and able to deliver the instrument tip with the necessary supplies. The micro-system is mounted on

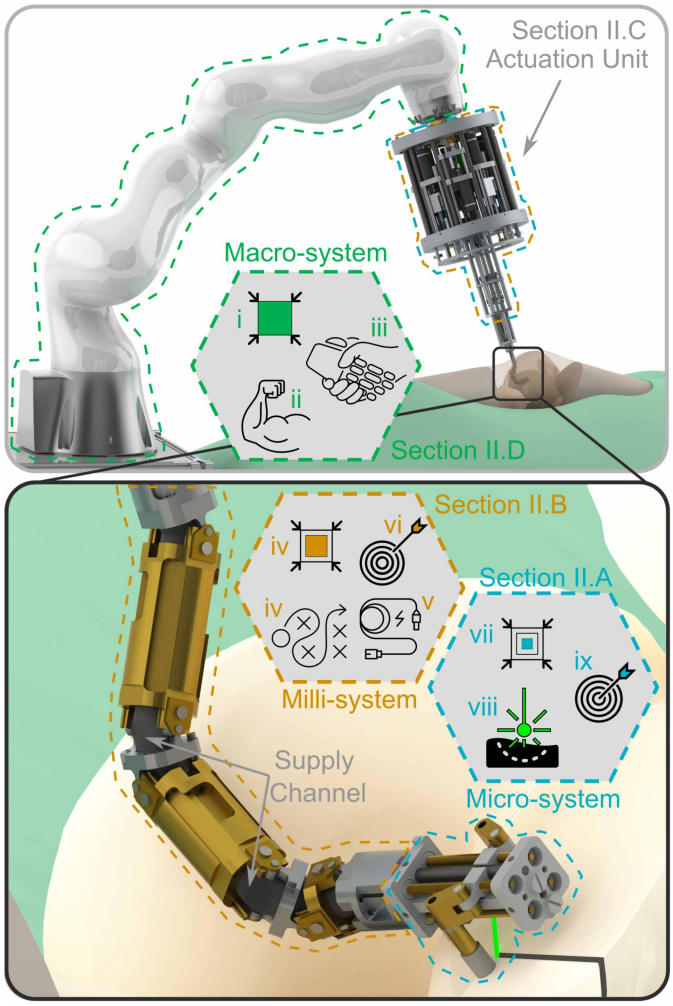

Fig. 1. Concept of the overall robotic system for laser osteotomy as a macro-milli-micro system: A serial robot (macro-system) is guiding a robotic endoscope (milli-system), which is inserted into the patient's knee. At the endoscope's tip, the micro-system accurately positions the surgical instrument, i.e., the laser. The peripherals of the milli- and micro-system that are necessary for actuation and control are located in the actuation unit outside the patient. The supply channel is housed inside the hollow core of the robotic endoscope and connects the micro-system with its peripheral components. The requirements depicted with logos in the tiles are explained in detail in the text with the corresponding roman index.

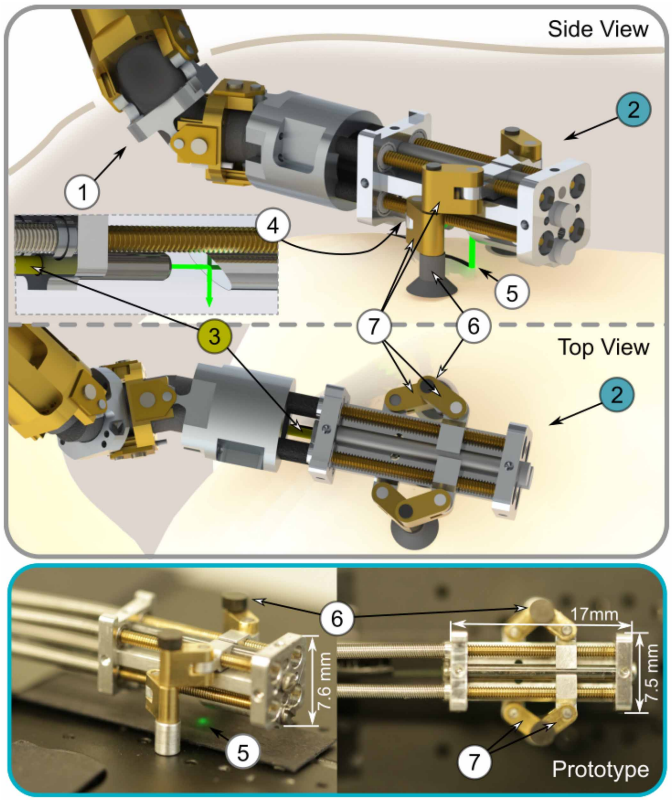

Fig. 2. The robotic endoscope (milli-system) ① is inserted into the knee joint. The cutting laser is guided through the endoscope to the micro-system ② by an optical fiber ③. The laser optics ④ redirect the laser beam ⑤, which then exits the micro-system perpendicular to its longitudinal axis towards the bone surface below the robot. The micro-system has two legs ⑥ whose positions are fixed relative to the bone surface. The micro-system consists of a parallel mechanism ⑦ that allows to move the laser optics in two translational and one rotational degrees of freedom.

the instrument tip and allows positioning the laser with the accuracy required for cutting and has minimal manipulation space requirements. The specific requirements for the individual subsystems deduced for our first application (UKA) are listed in the following sections (Sections II-A-II-D).

A. Micro-System—Miniature Parallel Robot

The micro-system needs to accurately guide the laser at the intervention site. Based on our currently envisioned diameter of the laser focal point of 0.5 mm [29], we aimed to achieve a positioning accuracy below 0.25 mm to enable the realization of continuous laser cuts based on point-wise ablation.

The micro-system was realized with a miniature parallel robot integrated at the endoscope tip. The laser light was guided through a fiber inside the robotic endoscope to the laser optics inside the miniature parallel robot. These laser optics redirected the laser to cut the bone below (Fig. 2). The miniature parallel robot was based on a 4-RRP parallel structure that enables to move the laser optics in three planar degrees of freedom (DoFs) with high accuracy. The miniature parallel robot attached to the target surface with two legs to increase stability and accuracy. Once attached, it had a workspace of approximately 34 mm^2 [28]. The legs' position relative to the bone could be fixed based on a non-invasive concept, e.g., suction cups [30] or balloon catheters. The topology of the miniature parallel robot allows for repositioning of the legs' attachment on the bone and thus "walk" along the bone surface [30]. After the first evaluation with an upscaled prototype [31], a miniature parallel robot prototype was built and showed sufficient positioning accuracy with a mean error of 0.07 mm [28]. The dimensions of the prototype were based on the manipulation volume that we expected to be available for a minimally invasive intervention inside the knee joint based on our previously performed cadaver experiments [10]. Space-consuming components of the miniature parallel robot, i.e., the laser for ablation and the motors and sensors for controlling the parallel robot, were placed externally. The mechanical power and the laser were transmitted from the peripheral components to the miniature parallel robot by means of flexible shafts and an optical fiber, respectively. The flexible shafts and the optical fiber were guided through the supply channel inside the hollow core of the milli-system.

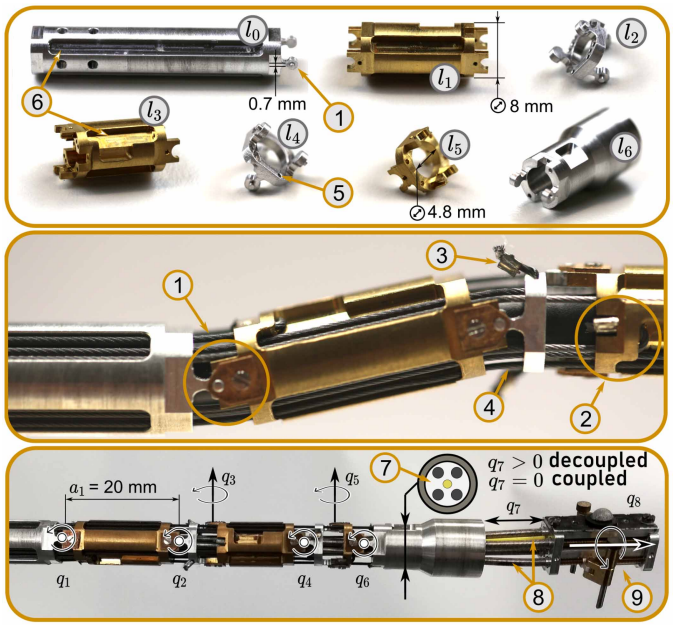

Fig. 3. The robotic endoscope consisted of seven rigid links (l_0–l_6) that were connected by six hinge joints ① (q_1-q_6). Two tendons were fixed on each rigid link by looping them back ② and adding an end stop (metal crimp) ③. The tendons ④ were guided through the walls of the rigid links. They entered and exited the links through corresponding holes ⑤. Grooves ⑥ were added to the links to decrease the needed depth for drilling the small holes. The supply channel ⑦ was guided through the hollow core of the robotic endoscope and provided the necessary supplies for actuation and intervention (i.e., flexible shafts and optical fiber ⑧) to the miniature parallel robot (micro-system) ⑨. The supply channel also allowed independent translation q_7 and rotation q_8 of the miniature parallel robot. The last link l_6 of the prototype is longer than required by the presented micro-system (and shown in Fig. 1 and 2) because the device was also used for prior experiments involving larger micro-system prototypes.

B. Milli-System—Robotic Endoscope and Supply Channel

The milli-system should deploy the miniature parallel robot (i.e., the micro-system) at the intervention site inside the patient's body. A positioning accuracy of the milli-system of at least 5 mm was required so that the targeted intervention site would lie within the range of operation of the miniature parallel robot and could be reached accurately. The milli-system should have a diameter of maximally 8 mm to allow minimally invasive insertion into the knee joint (based on our evaluation [10]). Also, the milli-system should have sufficient dexterity for reaching the bone-cutting locations for a standard UKA through a single skin incision. Furthermore, the milli-system should house the supply channel, i.e., the connection between the miniature parallel robot and its peripheral components. The supply channel needs to provide space for four flexible shafts (ø1.4 mm each) and a laser fiber (ø1 mm) for the current prototype.

The milli-system was realized as an articulated robotic endoscope with seven discrete links (Fig. 3). We chose an articulated approach in contrast to the often used continuous structure approaches (e.g., single or multi backbone approaches or concentric tube robots [32]) since it is less challenging to achieve robust and accurate shape estimation with an articulated structure [33]: A structure of discrete links enables the shape of the endoscope to be accurately determined by the known link lengths and joint angles, even when surrounding tissue is exerting contact forces on the endoscope. Thus, in the knee, where the environment is inhomogeneous, and a lot of contact with surrounding tissue is to be expected due to the narrow space conditions, articulated robots have conceptual advantages. Furthermore, we considered an articulated structure more suitable to realize small bending radii, which was considered necessary due to the narrow space conditions inside the knee. The joint lengths and joint axis arrangement of the prototype were designed iteratively, by tuning the kinematic structure of the endoscope and visually verifying with a knee phantom (VirtaMed ArthroS Knee, VirtaMed AG, Schlieren, Switzerland) that the resulting robotic endoscope was reaching the locations required for cutting bone in UKA. This approach does not guarantee that the resulting endoscope is suitable for performing UKA on a human knee with a single incision. However, we have taken this empirical approach for an initial prototype because there are still uncertainties regarding the workflow of the procedure. The design allowed us to obtain an endoscope with a realistic level of complexity, which is a first step in developing the surgical workflow and further optimize the kinematic endoscope structure.

To transmit necessary supplies to the miniature parallel robot, the robotic endoscope was constructed with a hollow core. This provides space for the supply channel that houses the flexible shafts, which are needed to actuate the miniature parallel robot (micro-system), as well as the optical fiber. The supply channel was rigidly connected to the miniature parallel robot, but could rotate and translate inside the hollow core along the robotic endoscope. Therefore, by translating and rotating the supply channel it was possible to translate and rotate (roll) the miniature parallel robot in additional two DoFs, which are independent of the robotic endoscope's movement and joint configuration. This independent rotation and translation further increases the endoscope's dexterity, which would have been challenging to implement by means of a corresponding motion of the endoscope's joints instead. The concept also allows a partial mechanical decoupling between the micro-system and the robotic endoscope once the micro-system is attached to the bone. The coupling can be realized by pulling back the micro-system via translating the supply channel ($q_7 = 0$, Fig. 3) to create a form-fit between the miniature parallel robot and the endoscope. The decoupling is realized by pushing the miniature parallel robot away from the endoscope, releasing the form-fit ($q_7 > 0$). In that state, the micro-system is only coupled to the milli-system by the flexible supply channel.

The rigid links were manufactured alternately of brass and aluminum. To maximize the diameter of the hollow core (4.8 mm) while minimizing the overall outer diameter (8 mm), i.e., allowing manufacturing a thin link wall (1.6 mm), we chose to implement hinge joints. These hinge joints were fixed along the joint axes by small laser cut plates with a thickness of 0.3 mm (custom parts, Waterjet AG, Aarwangen, Switzerland) manufactured out of bronze due to its good tribological properties and high stiffness. The position of the plate was fixed by a small pin and a screw (M0.7). The hinge joints allowed

TABLE I
DENAVIT HARTENBERG PARAMETERS

	Joint (i)	$\theta_i[rad]$	$d_i[mm]$	$a_i[mm]$	$\alpha_i[rad]$
Robotic Endoscope	1	q_1	0	20	0
	2	q_2	0	5	$-\pi/2$
	3	q_3	0	16.75	$\pi/2$
	4	q_4	0	5	$-\pi/2$
	5	q_5	0	5	$\pi/2$
	6	$\pi/2+q_6$	0	0	$\pi/2$
Supply Channel	7	0	19.75+q_7	0	0
	8	q_8	0	0	0

an angular deflection of ±30°. Each joint was controlled by two tendons (Tungsten strand with graphite coating to improve tribological properties, ø 0.5 mm, Fort Wayne Metals, IN, USA), according to an agonist-antagonist arrangement. The presented endoscope did not include integrated joint sensors, nor was space considered for adding such sensors. Instead, the joint angles were measured using an external tracking system (see Section II-E). We estimated that a rotation sensor with a diameter below 3 mm and a thickness below 2 mm would be required and we could not find a corresponding sensor. We consider the development and integration of such a sensor as a research topic by itself. Potential options are discussed in Section IV.

The endoscope consisted of six hinge joints in series and the supply channel allowed to move the miniature parallel robot in two additional degrees of freedom (Denavit Hartenberg parameters in the classical convention [34] are provided in Table I and the joints $q_1 - q_8$ are visualized in Fig. 3).

C. The Actuation Unit—Milli- and Micro-System Peripherals

The actuation unit should house all peripheral components for actuation and sensing necessary for controlling the milli-system (robotic endoscope) and the micro-system (miniature parallel robot).

The actuation unit consisted of various components which can be seen in Fig. 4. The micro-system actuation module ② was located in the center of the actuation unit and housed the four motors that actuate the flexible shafts transmitting the motion from the actuation unit, through the supply channel ① to the miniature parallel robot. The proximal, rigid part of the supply channel was rigidly attached to this module, while the distal, flexible part of the supply channel was rigidly connected to the miniature parallel robot (Fig. 4). The micro-system actuation module and the supply channel could be rotated and translated with respect to the remaining parts of the actuation unit by two supply channel actuation modules (③ and ④). The supply channel transmitted this translation and rotation to the miniature parallel robot at the tip of the robotic endoscope. The rotation is theoretically unlimited, but due to the wiring of the motors mounted in the micro-system actuation module and the integrated optical fiber, currently limited to a range of motion of about ±50°. For this reason, also the translation movement is currently limited to 10 mm. A detailed description of the technical realization of this module and its actuation is provided in the supplementary material.

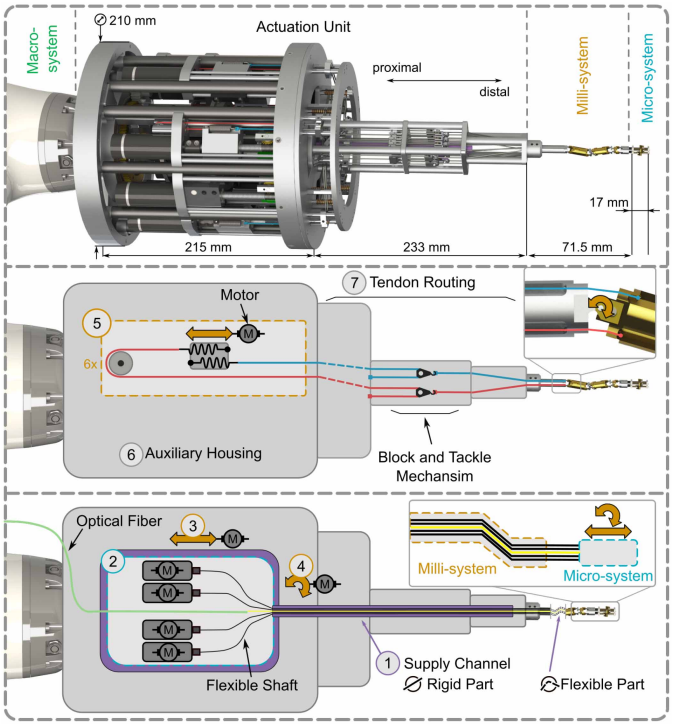

Fig. 4. The actuation unit housed all peripherals of the milli- and micro-system and was the anchorage of the supply channel ①. The actuation unit consisted of the micro-system actuation module ②, the translational ③ and rotational ④ supply channel actuation modules, six joint actuation modules ⑤, the auxiliary housing ⑥ that allowed mounting the actuation unit to the macro-system, and the tendon routing ⑦. The supply channel originated near the end effector of the macro-system and extended to the tip of the robotic endoscope. A technically more detailed figure of the actuation unit (including the tendon routing) is provided in the supplementary material.

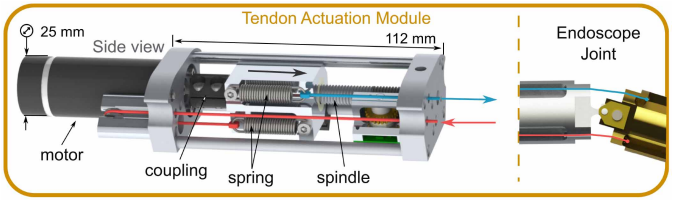

Fig. 5. Tendon actuation module: The joint motion of the six endoscope joints q_1-q_6 were actuated by one tendon actuation module each.

The joint actuation modules consisted of a lead screw driven by a DC motor (Maxon Motor AG, Sachseln, Switzerland) controlling the position of a linear slider along the motor axis. The absolute slider position was acquired by a magnetic single-turn rotational encoder coupled to the lead screw by means of a reduction drive. Each joint actuation module drove one joint of the endoscope by actuating two tendons, both of which are fixed to the module's linear slider. The agonistic tendon (Fig. 5 in blue) directly exited the actuation module in the direction of the endoscope, whereas the antagonistic tendon (red) was first guided into the opposite direction, where it was then rerouted towards the endoscope by a deviation pulley. This mechanism allowed the agonist-antagonist motion required to drive the endoscope's hinge joints to be implemented with a single lead screw and only a few mechanical parts. To provide compliance to the tendons and hence to the

endoscope joints, two linear springs were intercalated between the tendons and the slider.

The auxiliary housing module was devised to accommodate all actuation modules and to provide the necessary structural rigidity. The six tendon actuation modules and the two supply channel actuation modules were mounted circularly around the central micro-system actuation module. The modules were slid into the housing along linear rails and secured with a single pin each achieving a high level of modularity and ease of maintenance. The housing further supported cable management of all actuation modules and provided the mechanical interface to the macro-system.

The auxiliary tendon routing module consisted of a pyramidal structure to which the endoscope was mechanically attached and through which all twelve tendons were guided from the tendon actuation modules to the respective tendon entry holes at the first link (proximal end) of the endoscope. Each endoscope hinge joint was driven by two tendons emerging from a single tendon actuation module. The two tendon entry holes in the corresponding endoscope link were located diametrically opposed to one another. Thus, a number of deviation pulleys needed to be arranged to provide the twelve tendon paths from the tendon actuation modules to the endoscope. A block and tackle mechanism was integrated in the tendon routing module to transform the large travel range of the tendon actuation sliders to the smaller travel range of the endoscope hinge joints. This mechanism further allowed to split each tendon into two distinct parts, one ranging from the tendon actuation module to the block and tackle mechanism, and one from the mechanism to the endoscope joint, providing a way to dismount the endoscope and to tighten the tendons.

D. Macro-System—Serial Macro-Robot

The macro-system is needed for insertion and extraction movements of the robotic endoscope and for positioning the actuation unit during operation. It needs to carry the load of the actuation unit, robotic endoscope, and miniature parallel robot. It should have a large enough workspace to allow flexibility in placing the surgical system in the space-constrained operating room and to reliably realize the remote center of motion-type endoscope movements [35], [36]. Also, a large workspace might be required in procedures where distant surgical sites on the patient need to be treated during the same intervention (e.g., bone harvesting [37]). We considered the macro-system to require an accuracy in the order of millimeters to avoid extensive tissue strain at the endoscope's entry point. In addition, despite the large payload, the macro-system must be safe for physical human-robot interaction in the operating room and should provide interaction modes, such as telemanipulation or hand guidance to facilitate intuitive handling and reduce set-up time. Also, the macro-system must be controllable in a time-synchronized manner with the robotic endoscope.

Our current prototype was realized with a commercially available seven DoF serial robot, KUKA LBR iiwa 14 R820 (KUKA AG, Augsburg, Germany). This robot is certified with a repeatability of ± 0.15 mm [38] and would also be available in a medically certified version. Furthermore, it provides the necessary interfaces to realize safe custom time-synchronized control between the subsystems. It also allows safe human-robot interaction with speed limits and external torque detection. Furthermore, it is possible to extend the robot's workspace with an additional linear DoF [39]. Finally, the redundancy of the robot allows implementing intuitive null-space behavior [40], [41] that can help surgeons plan the surgery in the constrained space in the operating room.

E. Communication and Control

The control of the entire system is based on a central overall control (high-level control), which connects the various system components. This high-level control is realized in TwinCAT 3 running on an embedded computer CX2020 (both Beckhoff Automation GmbH Co. KG, Verl, Germany). The high-level controllers for all system components were integrated in this central control. The position and orientation of the system components measured with an optical tracking system were also fed into the high-level control directly (Fig. 6). Optical tracking of the robotic endoscope and the actuation unit was realized with a motion tracking system (Miqus M5 cameras, Qualisys AB, Gothenburg, Sweden). A total of six cameras were installed around the system and reflective markers were mounted on the system components to be tracked.

The high-level control communicated with the low-level control units of the individual system components, i.e., the KUKA controller (KUKA Sunrise Cabinet, KUKA AG), the motor drives (MAXPOS 50/5, Maxon Motor AG), and the digital and analog inputs and outputs (Beckhoff Automation GmbH) for the additional peripheral components in the actuation pack (e.g., brake, absolute rotary encoder).

The high-level control contained the control for the robot's motion. For the robotic endoscope, two main elements were included: state estimation and joint space controller. The state estimation calculated the current joint configuration of the robotic endoscope based on feedback from the optical tracking system and the endoscope kinematics. The feedback from the tracking system was necessary because the current prototype did not yet have integrated sensors for measuring the endoscope's joint angles. Thus, to estimate the robotic endoscope's current joint configuration, rigid tracking objects were placed on each endoscope link. Each rigid tracking object consisted of at least four individual markers that were tracked and allowed measuring the six DoF pose of the endoscope link on which it was mounted.

The joint space controller calculated the required change in tendon length based on the current and desired joint configuration of the robotic endoscope. From the required change in tendon length, the corresponding desired velocity signals for the motors were derived.

The rotation and translation movements of the supply channel were controlled with a P-controller. The current position of the supply channel was estimated using the sensor feedback from the motor encoders.

The control of the KUKA serial robot was also integrated into the high-level controller with a cascaded task space and

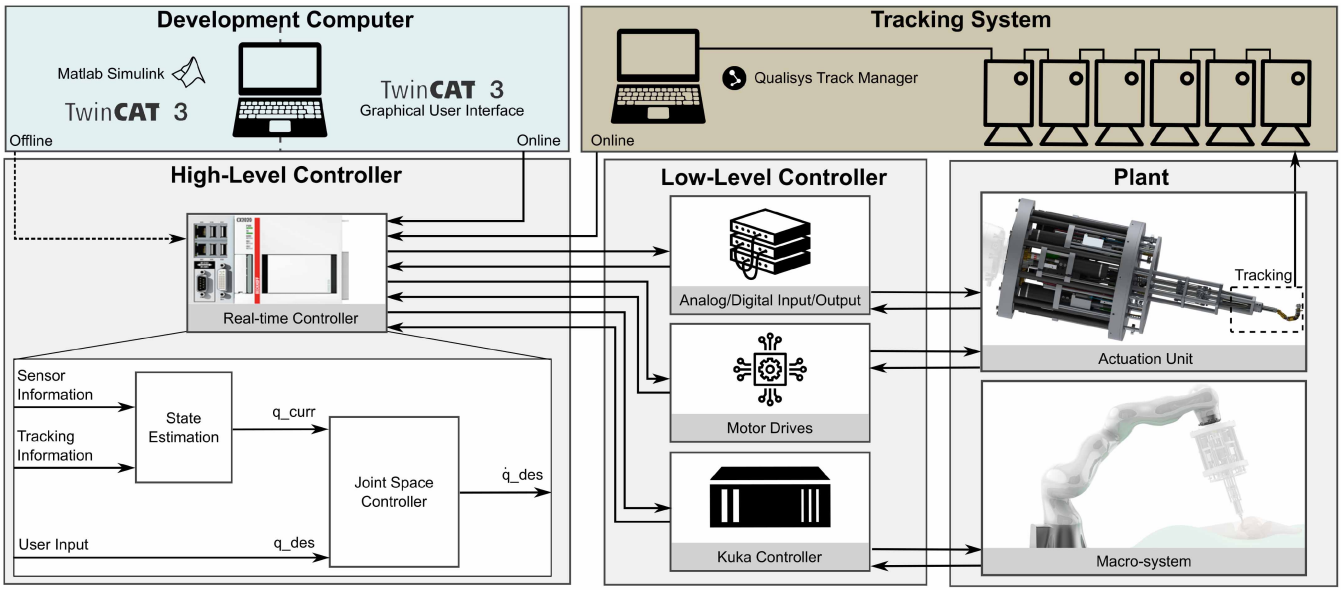

Fig. 6. Control architecture and communication of the system components. The optical tracking system was used for the joint position feedback of the robotic endoscope and experimental evaluation of the entire system and was directly integrated into the communication to ensure the correct synchronization of the data.

joint space control scheme. The resulting joint position commands were sent to the KUKA controller via the Fast Robot Interface (FRI). More detail on this control that synchronizes commands to the serial robot with additional hardware was published in previous work [39], [41].

F. Experimental Setup

To evaluate the system's performance and demonstrate its functionality, we measured and evaluated the robotic endoscope and supply channel movement during joint space path following experiments. For this purpose, the endoscope joint movements and the supply channel movements were measured and evaluated individually using the tracking system. During these experiments, the actuation unit was in an approximately horizontal position. In particular, we investigated the mutual influence of the endoscope joints' motion. Also, we tested the overall system functionality in an insertion-like motion on the test bench involving the serial robot and the robotic endoscope. In all experiments, the commanded and measured joint positions were recorded for evaluation.

1) Robotic Endoscope: We evaluated the endoscope joints (q_1 to q_6 in Table I) individually in separate experiments. During these experiments, the robotic endoscope's longitudinal axis was approximately horizontal, and the axes of joint 3 and 5 approximately vertical. At the beginning of each experiment, the endoscope was brought into the zero-configuration (straight). The rigid tracking object coordinate systems on each joint were rotated so that their axes were parallel. In each individual tracking experiment, one endoscope joint was commanded to move from 0° to 30°, to −30°, and back to 0°. The other joints were commanded to remain at 0°. Settling times at the joint positions 30° and −30°, were 2 min before continuing the movement.

The cable tensions for the joints proximal to the currently evaluated joint were increased to allow each joint to be evaluated individually, i.e., without the proximal joints' influence. The increased tension prevented unwanted movement of the proximal joints. The distal joints needed to move with the current joint in order to maintain the 0° joint position. Steps of 2.5° were taken between the main steps of 30°. These intermediate steps were necessary due to the mutual influence of the joint movements. In each of these intermediate steps, we waited until all joint errors were below 1°, or 1 min had elapsed to allow observing long-term effects. Also, we conducted an experiment, where all joints were simultaneously commanded to move from 0° to 5°, to −5° and back to 0°.

2) Supply Channel: We evaluated the translational and rotational motion of the supply channel (q_7 and q_8 in Table I) and how this motion is transferred to the micro-system, i.e., the miniature parallel robot. The supply channel's current position and rotation were estimated based on the actuation unit's encoder feedback. This estimated position and rotation were used for control. For evaluation, the position and rotation of the miniature parallel robot were measured using the tracking system. For this purpose, we placed a rigid tracking object on the miniature parallel robot to measure its position with respect to the last link of the robotic endoscope. A linear movement and a rotational movement of the supply channel from 0 mm to 10 mm and from 0° to 100°, respectively, were commanded in succession. The supply channel was commanded to move to the reference and back to the origin. When the estimated position or rotation reached the reference position, we waited for 10 sec before moving back. The robotic endoscope was positioned in the zero-configuration (straight) during these experiments.

3) Overall System: A joint path was specified for the robotic endoscope and the serial robot to qualitatively verify the overall system's functionality (Fig. 7). The movement

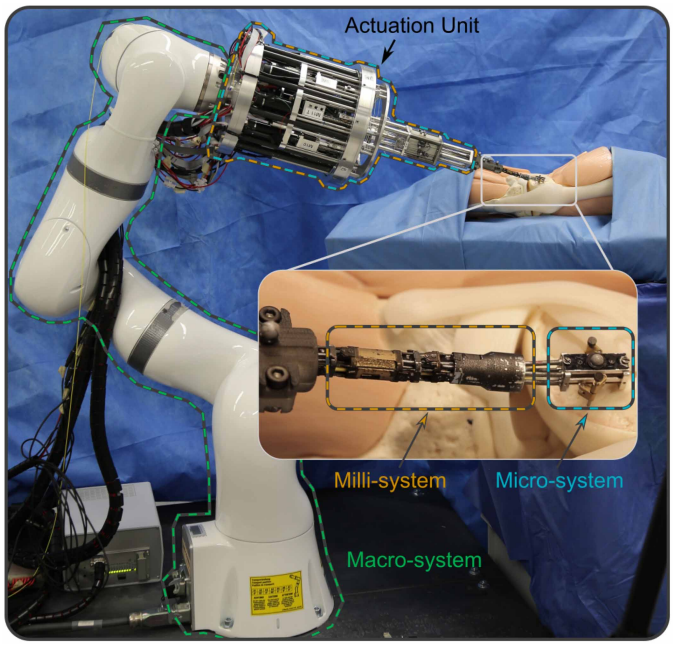

Fig. 7. Experimental setup of the overall macro-milli-micro system. The rigid tracking objects on the robotic endoscope were removed for this image.

resembled an insertion movement, including bending of the endoscope's last two joints (q_5 and q_6) during the last part of the motion in free space.

G. Experimental Evaluation

1) Robotic Endoscope: The desired and measured motions of the individually deflected endoscope joints and the corresponding distal joints were recorded. The deviation of the measured endoscope movement from the commanded movement, i.e., the tracking error, was calculated and analyzed. The settling error was calculated for each individual tracking experiment at 30° and −30°. The settling error was defined as the maximum tracking error from the reference value during 30 sec after the joint followed the reference value for 90 sec. The robotic endoscope's tip tracking errors were calculated based on the measured joint tracking errors using the endoscope's kinematics.

2) Supply Channel: The commanded, estimated, and tracked motions of the miniature parallel robot during translation and rotation of the supply channel were evaluated. The estimated position and rotation represented the supply channel's state inside the actuation unit (Fig. 4) as estimated by the control system using the encoder feedback. The tracked motion referred to the resulting translation and rotation of the miniature parallel robot at the tip of the robotic endoscope measured by the tracking system. The settling error between the commanded and tracked motions was calculated as the maximal tracking error during a time period of 5 sec before the reference was changed.

3) Overall System: The coordinated joint motion of the robotic endoscope and the serial robot was video recorded. The deviation of the measured joint movement from the commanded movement, i.e., the tracking error, was calculated. The joint positions of the serial robot were provided by the KUKA controller and the joint positions of the robotic endoscope were calculated based on the tracking system feedback (as during the robotic endoscope tracking experiments).

III. Results

A. Robotic Endoscope

The individual joint tracking experiments for joints q_2-q_6 were successfully performed and the joints were able to follow the commanded steps (Fig. 8). Joint 1 was damaged during experiments and could not be evaluated. Joint 5 had the highest settling error (Fig. 8).

The collective movement of all endoscope joints to ±5° could be successfully performed (Fig. 9(a)). The tracking errors seem to increase for more distal joints (Fig. 9(b)). The endoscope's tip settling error were approximately 0.6 mm at 5° and 1.2 mm at −5°.

B. Supply Channel

The settling error of the translation when commanding a movement of the supply channel (q_7) from 0 mm to 10 mm was 0.2 mm. Driving back resulted in a settling error of 1.1 mm. The settling error of the rotation (q_8) when commanding a rotation of from 0° to 100° was 10°, and 82° when driving back to 0° (Fig. 10).

C. Overall System

The insertion-like motion of the serial robot and the robotic endoscope on the test bench was carried out successfully. The serial robot followed its intended position, while the robotic endoscope showed settling errors comparable to the endoscope tracking experiments (Fig. 11). A movie recording of the motion is available as supplementary material.

IV. Discussion

The experimental evaluation of the robotic endoscope showed that the control of individual joints with the herein presented mechanical design and control system was possible with a settling error below 1° (Fig. 8) and a tip settling error of 0.5 mm. This meets in principle our current requirements for the positioning accuracy of the robotic endoscope. In particular, the mutual influence of the joints could be successfully handled and the feasibility of an articulated robotic endoscope control that allows reasonably accurate joint and tip control could be demonstrated. However, the results also showed that the joint tracking errors during the endoscope's motion are bigger than the joint settling error (e.g., up to 7° for joints 5 and 6 in Fig. 8(e)). The tracking errors also tended to increase as more joints were involved in the endoscope movement (Fig. 8). In the experiment, where all joints were moved in a coordinated motion, the tracking errors were larger than in the individual joint tracking experiments (Fig. 9(a)), and the most distal joint (joint 6) showed the largest tracking errors (Fig. 9(b)).

The joint tracking errors were mainly composed of the following error sources:

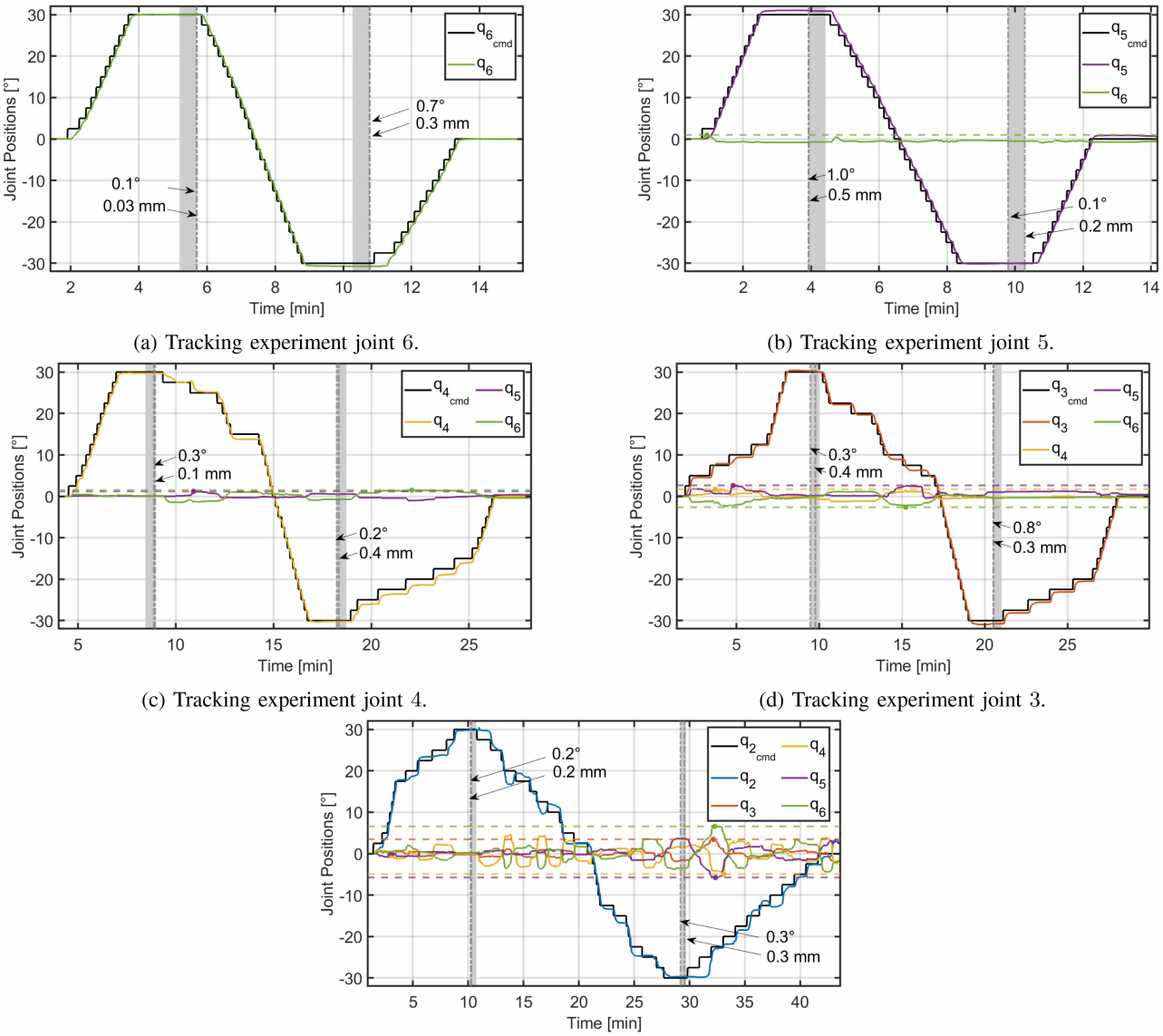

(a) Tracking experiment joint 6.

(b) Tracking experiment joint 5.

(c) Tracking experiment joint 4.

(d) Tracking experiment joint 3.

(e) Tracking experiment joint 2.

Fig. 8. Endoscope joint tracking performance: Joint positions (q_i) measured with the tracking system during the evaluation of one individual joint. More distal joints were commanded to hold their position at 0° and were plotted to indicate their parasitic motion. More proximal joints were not plotted since they were held at 0° with higher tendon pretension. The maximal joint tracking error of the distal joints and the maximal endoscope tip tracking error are indicated with a horizontal dashed line. The gray area indicates the 30 sec in which the settling error was calculated. The joint and tip settling errors are stated and their location is indicated with a vertical dashed line.

- Hysteresis in the elastic elements of the drive trains (i.e., springs and tendons). For example, if an endoscope joint overshot the desired joint position, the previously pulling tendon's linear spring had to be unloaded first and the linear spring of the newly pulling tendon had to be loaded before the joint could move in the other direction (e.g., Fig. 9(a) between 1.8 and 2.3 min).
- The dependence of the distal joints on the proximal joints resulted in settling delays for the distal joints. For example, deflections of joint 5 caused disruptive movements in joint 6 since the deflection of joint 5 also affected the tendons that actuate joint 6 (Fig. 8(b)).
- The manual tensioning of tendons and the resulting non-repeatable and unevenly distributed stresses in the system.
- The limited accuracy of the tracking system and the fabrication, assembly, and positioning of the rigid body markers.
- Dependency on the reference input (in our case non-continuous input steps and step size).

The joint settling error demonstrated that it is possible to control the robotic endoscope with a joint accuracy of approximately 1°. We interpret this settling error as a lower bound for the achievable tracking performance. Based on the observed tracking errors of up to 7°, we believe that there is room to improve tracking performance by means of control and modeling. We see the modeling of the hysteresis as the most promising approach. In our experience, the friction in each tendon drive train depends on the robotic endoscope's current

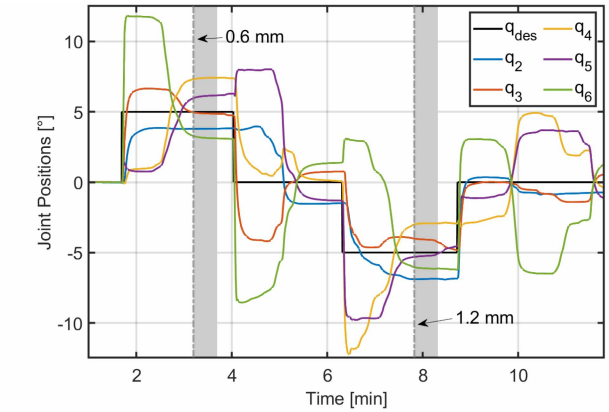

(a) Joint positions measured with the tracking system. The gray area indicates the 30 sec in which the settling error was calculated. The tip settling errors are stated and their location is indicated with a vertical dashed line.

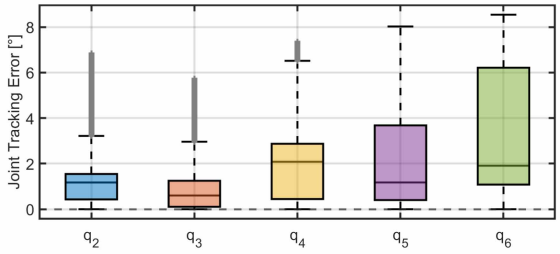

(b) On each box, the central mark, bottom and top edges indicate the median, the 25th, and 75th percentiles, respectively. The dashed lines extend to the most extreme data points not considered outliers, and the outliers are plotted individually with the + symbol.

Fig. 9. Experiment when all joints were commanded to move to ±5°.

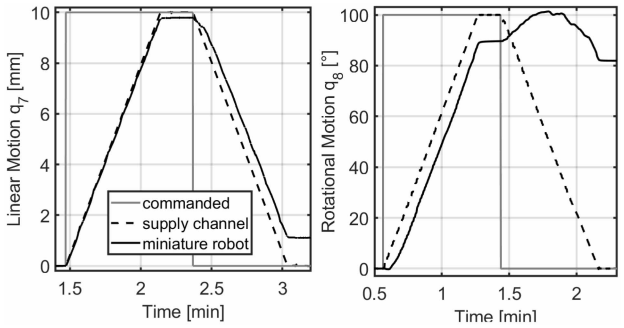

Fig. 10. Translation and rotation of the miniature parallel robot motion actuated by the supply channel.

joint configuration and the resulting stresses in the tendons and pressure on the hinge joints. Accordingly, we see it as a challenge to model the hysteresis of the motion transmission from motor to joint and instead suggest installing an additional sensor system to measure the linear springs' deflection.

The implementation of the milli-system as an articulated tendon-driven robotic endoscope seems promising but challenging in terms of actuation. The robotic endoscope's tracking performance could be further improved if two motors were provided for each joint, i.e., one motor for each tendon. This could enable controlling the joints even more accurately since the agonist tendon could be controlled independently of the antagonist tendon. Also, using serial elastic actuation (SEA)

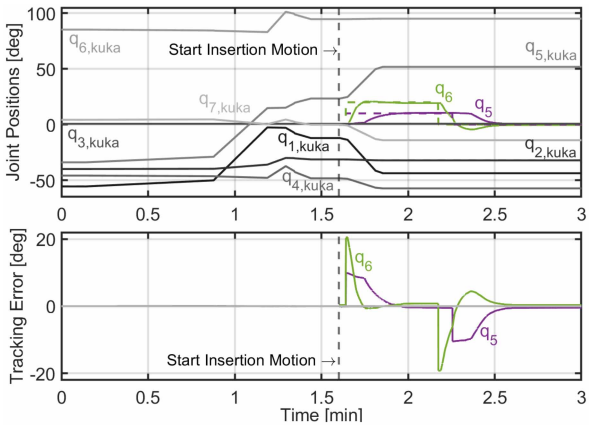

Fig. 11. Synchronized control of the robotic endoscope and the serial robot during the insertion-like motion on the test bench. Top: The solid lines indicate the serial robot joint positions [$q_{1,kuka}$ (proximal joint, robot base)−$q_{7,kuka}$ (distal joint, robot flange)] and the robotic endoscope joint positions [$q_5 - q_6$]. The colored dashed lines indicate the commanded endoscope joint positions. Bottom: The solid lines indicate tracking errors of robotic endoscope joints.

for the tendon actuation would allow varying the stiffness of the individual endoscope joints [42]. Variable stiffening of the endoscope joints could reduce inter-joint dependencies and improve the accuracy of the robotic endoscope. For example, using SEA, a control strategy could be implemented in which the endoscope joints are stiffened successively from proximal to distal when they have reached the desired joint position. Also, the tendons' tensioning, currently done manually with the block and tackle mechanism, could be performed with greater accuracy, repeatability, and automation. SEA would also open up the estimation of torques in the endoscope joints. Known joint torques could be used to improve safety or provide haptic feedback to the surgeon [42]. However, two motors per joint and the installation of SEA elements would increase the actuation unit's volume, price, weight, and might make the handling of the device more difficult.

The observed tip positioning accuracy indicated by the joint settling errors of the presented articulated tendon-driven robotic endoscope is comparable to other presented devices based on a continuous structure [33]. Although the actuation of the robotic endoscope, with an articulated tendon-driven structure consisting of rigid links and discrete joints, seems more complex than comparable devices with continuum mechanics, we see important conceptual advantages: For example, state estimation, modeling, and control of the system can be realized with high accuracy independent of the environment homogeneity. Also, the robotic structure can be realized in such a way that greater forces can be exerted on the environment without deformation of the endoscope's structure. However, the segment-based design of the endoscope contains many individual parts, and we, therefore, expect that the manufacturing and cleaning of our robotic joint endoscope could become challenging.

The robotic endoscope presented was controlled based on optical tracking of the endoscope links. For minimally invasive applications, another measurement method of the robotic endoscope links must be found as a direct line of sight will not

be available. We consider accurate estimation of joint angles based on tendon length to be unrealistic due to the unfavorable conversion of tendon length change to joint angle change, play in the tendon guidance, and elasticities in the tendons. Also, direct measurement of the joint angles would be safer to measure the instantaneous endoscope joint configuration. Possible joint angle tracking solutions would be electromagnetic tracking (e.g., Aurora, NDI, Waterloo, Canada) or the integration of dedicated miniature sensors. Electromagnetic tracking would be challenging due to the disturbances caused by the robotic system, i.e., the serial KUKA robot, the actuation unit, and the robotic endoscope. Dedicated miniature joint sensors are challenging to be built due to the small dimensions required. For the current endoscope design we estimate that a sensor with a diameter below 3 mm with a thickness below 2 mm would be required to allow integration. A concept of a joint sensor has been proposed [43] but the miniaturization still needs to be shown. The above mentioned conceptual advantages in state estimation, modeling, and control highly depend on the successful estimation of joint angles.

The robotic endoscope prototype was fragile due to the small structures made of relatively soft metal (i.e., aluminum and brass). One of the hinge joints in the first endoscope joint was damaged during the experiments. We assume that due to a slight tilt in the hinge joint, the compressive forces on the joint, which arise from the tendons' tension and are highest in the first joint, led to a deformation of the thin hinge neck (width of 0.7 mm). Realizing the joints with miniature ball bearings with integrated joint axes (e.g., the SD 1467XZRY by MPS Watch, Bonfol, Switzerland) might be a more robust alternative that would also reduce the friction in the joints.

The translation of the miniature parallel robot by translating the supply channel inside the actuation unit resulted in a settling error of 1.1 mm. Whereas the rotation of the miniature parallel robot by rotating the supply channel inside the actuation unit resulted in a settling error of 10° in one direction and failed in the other direction. The accuracy of the translation motion would be sufficient provided that a sensor is included to measure the translation position of the miniature parallel robot and allow correcting tracking errors via closed-loop control. We assume that the rotation failure could be caused by a compression or twisting of the supply channel's flexible part, which consisted of the flexible shafts and the optical fiber.

The main limitation of the transmission of the supply channel's movement from inside the actuation unit to the miniature parallel robot is the lack of a suitable element to transmit, in particular, the rotational movement through the flexible part of the supply channel inside the robotic endoscope. Motion transmission in the flexible part of the supply channel could be improved using a flexible tube with surface reinforcements inhibiting longitudinal compression and twisting of the tube around the longitudinal axis. However, such a tube would represent an additional resistance for the bending movements of the robotic endoscope. The transmission of the supply channel's movement also needs to be verified in curved joint configurations of the endoscope. Thus, we plan to manufacture the supply channel similar to flexible shafts, i.e., based on wire wound into coils twisted alternately in clock-wise and counterclock-wise direction. Such a design offers torsional stiffness while maintaining bending flexibility. Based on our experience with rotary transmissions for the actuation of micro-systems, we consider this concept promising. However, the correct dimensioning of the supply channel and the hollow core of the endoscope requires further iterations of the prototype to continue to allow undisturbed bending of the robotic endoscope. The two additional degrees of freedom (q_7 and q_8) for placing the micro-system at the target location independently of the endoscope's joint configuration could be a great advantage. For example, an intervention on opposite regions, e.g., in the joint gap, could be realized without movement of the endoscope by rotating only the miniature robot. By developing a tube for the flexible part of the supply channel and integrating sensors to measure the miniature parallel robot's position and rotation, it should be possible to realize the motion transmission of the supply channel successfully.

The overall system was successfully built and put into operation. The three system components, i.e., macro-, milli-, and micro-system could be integrated into a common central control system. We successfully demonstrated that the macro-system and the milli-system could be controlled together and perform an insertion-like motion in free air (Fig. 11). Selecting the macro-milli-micro approach reduces the requirements on the individual subsystems. However, the interaction and synchronization of the individual subsystems add a certain degree of additional complexity. Depending on the further development of the surgical workflow, it is conceivable that individual system components can be simplified again in a subsequent iteration of system development based on specific surgeon requirements. For example, manual insertion of the micro-system using a flexible endoscope could be considered.

Since minimally invasive UKA using laser osteotomy is a novel procedure, which also requires advances in other research fields, such as laser physics or surgical navigation, the requirements for the robotic system were developed iteratively and were based on initial assumptions about a possible surgical workflow. Thus, the presented robotic endoscope's kinematic structure is based on these assumptions and visual verification using a knee phantom. To which extent the current endoscope design will be able to mechanically perform the intervention in a human knee has not yet been determined. However, since the final workflow for minimally invasive UKA using laser osteotomy is primarily influenced by other system components and their limitations (e.g., the cutting laser), we consider the design presented here to be good enough for technology demonstration. Optimization of the endoscope structure does not appear to be target-oriented before the final workflow is determined.

We have successfully demonstrated a first prototype of a robotic system based on the macro-milli-micro approach. The system functions in principle and could allow the positioning and supply of a miniature parallel robot for laser positioning in the context of minimally invasive interventions in future. Compared to existing robotic devices for laser applications in medicine, we show the first approach that aims at the minimally invasive cutting of bones and will allow manipulating a laser instrument in the narrow manipulation space

above bones. To the best of our knowledge, a similar device has not yet been presented. In order to realize the minimally invasive cutting of bones with the presented system, further development steps are necessary, such as the integration of a high-power laser and the development of a motion planner that enables the planning of the insertion motion of the macro- and milli-system into the patient. To show the presented system's clinical feasibility, experiments need to be performed in a more realistic setting (i.e., minimally invasive insertion in a phantom or cadaver). However, the milli- and micro-system components must be more robustly manufactured and protected from contamination to allow such experiments. Also, a joint measurement technique that does not require a direct line of sight must be implemented to control the endoscope motion accurately.

V. Conclusion

We have introduced the mechanical part of a robotic system for future application in minimally invasive laser osteotomy based on the macro-milli-micro approach. Compared to existing systems for laser osteotomy, our system was designed to allow minimally invasive insertion and guidance of an optical fiber for bone cutting inside narrow cavities, such as inside the knee joint, with minimal manipulation space requirements.

The presented tendon-driven, articulated robotic endoscope was based on individually controllable discrete joints (milli-system). With appropriate sensing, this approach preserves the conceptual advantages of accurate shape estimation independent of the environment and the use of well-established serial manipulator control strategies. We successfully demonstrated the functionality and evaluated the tracking accuracy of the robotic endoscope and could show that it is possible to control the individual joints with a settling error below 1°, despite the mutual influence of the distal joints' motion on the proximal joints. To achieve this tracking accuracy generally and also with multi joint movements, it will be necessary to measure the hysteresis in the elastic components of the drive train. Also, the integration of series elastic actuation and two motors per joint (one motor per tendon) would open up promising new possibilities such as automatic and repeatable tensioning of the tendons or the implementation of control strategies in which the stiffness of individual joints is selectively adapted.

The robotic endoscope was implemented with a large hollow core (core diameter of 4.8 mm and an endoscope wall thickness of 1.6 mm) that comprises a flexible supply channel for the micro-system or would allow passage of other surgical tools. The translation of the micro-system actuated by the supply channel, independent of the robotic endoscope, was successfully demonstrated, while the rotation still needs improvement.

The robotic endoscope and the serial manipulator (macro-system) have completed a first time-synchronized insertion-like motion on the test bench. With this work, we could demonstrate that the designed robotic mechanical system can be expected to be suitable for the overall realistic system implementation for the envisioned minimally invasive laser osteotomy.

Acknowledgment

The authors thank Prof. Dr. med. Niklaus F. Friederich for his continuous support concerning medical questions. They also thank Frédéric Bourgeois, who contributed to the actuation unit's design and control, and Flin Höpflinger, who contributed to the robotic endoscope's kinematic structure within the scope of his semester thesis. They would also like to thank Sascha Martin and his team at the Physics Workshop at the University of Basel for their support in manufacturing the prototype. The authors have no conflict of interest to disclose.

References

[1] M. Augello, W. Deibel, K. Nuss, P. Cattin, and P. Jürgens, "Comparative microstructural analysis of bone osteotomies after cutting by computer-assisted robot-guided laser osteotome and piezoelectric osteotome: An in vivo animal study," *Lasers Med. Sci.*, vol. 33, no. 7, pp. 1471–1478, Sep. 2018.

[2] J. J. Kuttenberger *et al.*, "Computer-guided CO2-laser osteotomy of the sheep tibia: Technical prerequisites and first results," *Photomed. Laser Surg.*, vol. 26, no. 2, pp. 129–136, Apr. 2008.

[3] J. Burgner, M. Müller, J. Raczkowsky, and H. Wörn, "Ex vivo accuracy evaluation for robot assisted laser bone ablation," *Int. J. Med. Robot. Compu. Assist. Surg.*, vol. 6, no. 4, pp. 489–500, Dec. 2010.

[4] J. Burgner, M. Mueller, J. Raczkowsky, and H. Woern, "Robot assisted laser bone processing: Marking and cutting experiments," in *Proc. Int. Conf. Adv. Robot.*, Jul. 2009, pp. 1–6.

[5] Computer assisted surgery apparatus and method of cutting tissue, by P. Cattin, M. Griessen, A. Schneider, and A. Bruno. (2013, Jul. 1). European Patent 2 821 024. Accessed: Mar. 11, 2021. [Online]. Available https://patentscope.wipo.int/search/en/detail.jsf?docId=EP128596547

[6] D. Kundrat *et al.*, "Preclinical performance evaluation of a robotic endoscope for non-contact laser surgery," *Ann. Biomed. Eng.*, vol. 49, no. 2, pp. 585–600, Feb. 2021.

[7] M. Zhao, T. J. C. O. Vrielink, A. A. Kogkas, M. S. Runciman, D. S. Elson, and G. P. Mylonas, "LaryngoTORS: A novel cable-driven parallel robotic system for transoral laser phonosurgery," *IEEE Robot. Autom. Lett.*, vol. 5, no. 2, pp. 1516–1523, Apr. 2020.

[8] M. S. Erden, B. Rosa, N. Boularot, B. Gayet, G. Morel, and J. Szewczyk, "Conic-spiraleur: A miniature distal scanner for confocal microlaparoscope," *IEEE/ASME Trans. Mechatronics*, vol. 19, no. 6, pp. 1786–1798, Dec. 2014.

[9] P. A. York, R. Peña, D. Kent, and R. J. Wood, "Microrobotic laser steering for minimally invasive surgery," *Sci. Robot.*, vol. 6, no. 50, Jan. 2021, Art. no. eabd5476.

[10] M. Eugster *et al.*, "Quantitative evaluation of the thickness of the available manipulation volume inside the knee joint capsule for minimally invasive robotic unicondylar knee arthroplasty," *IEEE Trans. Biomed. Eng.*, vol. 68, no. 8, pp. 2412–2422, Aug. 2021.

[11] "The burden of musculoskeletal conditions at the start of the new millennium," WHO Sci. Group, World Health Org., Geneva, Switzerland, Rep. 919, 2003.

[12] J. Bertrand, *DE Erkrankungen des Immunsystems, des Bindegewebes und der Gelenke*, 20th ed. Berlin, Germany: ABW Verlag, Apr. 2020, pp. 3256–3264.

[13] K. Yang, M. Wang, S. Yeo, and N. Lo, "Minimally invasive unicondylar versus total condylar knee arthroplasty-early results of a matched-pair comparison," *Singapore Med. J.*, vol. 44, no. 11, pp. 559–562, Nov 2003.

[14] S. Bengtson and K. Knutson, "The infected knee arthroplasty: A 6-year follow-up of 357 cases," *Acta Orthopaedica Scandinavica*, vol. 62, no. 4, pp. 301–311, Aug. 1991.

[15] M. S. Noticewala, J. A. Geller, J. H. Lee, and W. Macaulay, "Unicompartmental knee arthroplasty relieves pain and improves function more than total knee arthroplasty," *J. Arthroplasty*, vol. 27, no. 8, pp. 99–105, 2012.

[16] C. T. Laurencin, S. B. Zelicof, R. D. Scott, and F. C. Ewald, "Unicompartmental versus total knee arthroplasty in the same patient. A comparative study," *Clin. Orthop. Related Res.*, vol. 273, pp. 151–156, Dec. 1991.

[17] J. Newman, R. Pydisetty, and C. Ackroyd, "Unicompartmental or total knee replacement: The 15-year results of a prospective randomised controlled trial," *J. Bone Joint Surg. British Vol.*, vol. 91, no. 1, pp. 52–57, May 2009.

[18] O. Robertsson, L. Borgquist, K. Knutson, S. Lewold, and L. Lidgren, "Use of unicompartmental instead of tricompart-mental prostheses for unicompartmental arthrosis in the knee is a cost-effective alternative: 15,437 primary tricompartmental prostheses were compared with 10,624 primary medial or lateral unicompartmental prostheses," *Acta Orthopaedica Scandinavica*, vol. 70, no. 2, pp. 170–175, Jan 1999.

[19] J. Plate *et al.*, "Unicompartmental knee arthroplasty: Past, present, future," *Reconstruct. Rev.*, vol. 2, no. 1, pp. 52–62, Aug. 2012.

[20] W. G. Hamilton, M. B. Collier, E. Tarabee, J. P. McAuley, C. A. Engh, and G. A. Engh, "Incidence and reasons for reoperation after minimally invasive unicompartmental knee arthroplasty," *J. Arthroplasty*, vol. 21, no. 6, pp. 98–107, Sep. 2006.

[21] P. Hernigou and G. Deschamps, "Alignment influences wear in the knee after medial unicompartmental arthroplasty," *Clin. Orthop. Related Res.*, vol. 423, pp. 161–165, Jun. 2004.

[22] J. N. Weinstein, T. P. Andriacchi, and J. Galante, "Factors influencing walking and stairclimbing following unicompartmental knee arthroplasty," *J. Arthroplasty*, vol. 1, no. 2, pp. 109–115, Oct. 1986.

[23] P. Barbadoro *et al.*, "Tibial component alignment and risk of loosening in unicompartmental knee arthroplasty: A radiographic and radiostereometric study," *Knee Surg. Sports Traumatol. Arthroscopy*, vol. 22, no. 12, pp. 3157–3162, Dec. 2014.

[24] S. Stübinger *et al.*, "Comparison of Er:YAG laser and piezoelectric osteotomy: An animal study in sheep," *Lasers Surg. Med.*, vol. 42, no. 8, pp. 743–751, Oct. 2010.

[25] L. M. B. Bernal, F. Canbaz, N. F. Friederich, P. C. Cattin, and A. Zam, "Measurements of coupling efficiency of high power Er:YAG laser in different types of optical fibers," in *Proc. Opt. Fibers Sens. for Med. Diagn. Treatment Appl.*, vol. 11233, Feb. 2020, pp. 178–183.

[26] L. M. B. Bernal *et al.*, "Optical fibers for endoscopic high-power Er: Yag laserosteotomy," *J. Biomed. Opt.*, vol. 26, no. 9, Sep. 2021, Art. no. 95002.

[27] H. Abbasi *et al.*, "Combined Nd:YAG and Er:YAG lasers for real-time closed-loop tissue-specific laser osteotomy," *Biomed. Opt. Exp.*, vol. 11, no. 4, pp. 1790–1807, Apr 2020.

[28] M. Eugster, J.-P. Merlet, N. Gerig, P. C. Cattin, and R. Georg, "Miniature parallel robot with submillimeter positioning accuracy for minimally invasive laser osteotomy," *Robotica*, vol. 40, no. 4, p. 1–28, Aug. 2021.

[29] L. M. B. Bernal *et al.*, "Optimizing controlled laser cutting of hard tissue (bone)," *Automatisierungstechnik*, vol. 66, no. 12, pp. 1072–1082, Nov. 2018.

[30] M. Eugster, M. O. Barros, P. C. Cattin, and G. Rauter, "Design evaluation of a stabilized, walking endoscope tip," in *Proc. Int. Workshop Med. Service Robots*, vol. 93, Nov. 2020, pp. 127–135.

[31] M. Eugster, P. C. Cattin, A. Zam, and G. Rauter, "A parallel robotic mechanism for the stabilization and guidance of an endoscope tip in laser osteotomy," in *Proc. IEEE/RSJ Int. Conf. Intell. Robots Syst. (IROS)*, Oct. 2018, pp. 1306–1311.

[32] J. Burgner-Kahrs, D. C. Rucker, and H. Choset, "Continuum robots for medical applications: A survey," *IEEE Trans. Robot.*, vol. 31, no. 6, pp. 1261–1280, Dec. 2015.

[33] C. Shi *et al.*, "Shape sensing techniques for continuum robots in minimally invasive surgery: A survey," *IEEE Trans. Biomed. Eng.*, vol. 64, no. 8, pp. 1665–1678, Aug. 2017.

[34] J. Denavit and R. S. Hartenberg, "A kinematic notation for lower-pair mechanisms based on matrices," *ASME J. Appl. Mech.*, vol. 6, pp. 215–221, Jun. 1955.

[35] J. Sandoval, G. Poisson, and P. Vieyres, "A new kinematic formulation of the RCM constraint for redundant torque-controlled robots," in *Proc. IEEE/RSJ Int. Conf. Intell. Robots Syst. (IROS)*, Sep. 2017, pp. 4576–4581.

[36] H. Su, S. Li, J. Manivannan, L. Bascetta, G. Ferrigno, and E. D. Momi, "Manipulability optimization control of a serial redundant robot for robot-assisted minimally invasive surgery," in *Proc. IEEE Int. Conf. Robot. Autom. (ICRA)*, May 2019, pp. 1323–1328.

[37] K. J. Zouhary, "Bone graft harvesting from distant sites: Concepts and techniques," *Oral Maxillofacial Surg. Clin.*, vol. 22, no. 3, pp. 301–316, Aug. 2010.

[38] *Robots, LBR iiwa, LBR iiwa 7 R800, LBR iiwa 14 R820, Specification, Spez LBR iiwa V4*, KUKA Lab. GmbH, Augsburg, Germany, Oct. 2014, p. 17.

[39] M. Karnam, P. Cattin, G. Rauter, and N. Gerig, "Comparing cascaded real-time controllers for an extended KUKA LBR iiwa robot during physical human-robot interaction," in *Proc. Siebte IFToMM D-A-CH Konferenz*, Feb. 2021, p. 2.

[40] M. Karnam, R. Parini, M. Eugster, P. Cattin, G. Rauter, and N. Gerig, "An intuitive interface for null space visualization and control of redundant surgical robots," *Proc. Autom. Med. Eng.*, vol. 1, no. 1, p. 2, Feb. 2020.

[41] M. Karnam *et al.*, "Learned task space control to reduce the effort in controlling redundant surgical robots," in *New Trends in Medical and Service Robotics*. Cham, Switzerland: Springer, Nov. 2021, pp. 161–168. [Online]. Available: https://link.springer.com/chapter/10.1007/978-3-030-58104-6_19

[42] L. Fasel, N. Gerig, P. C. Cattin, and G. Rauter, "Tendon force control evaluation for an endoscope with series elastic actuation," in *New Trends in Medical and Service Robotics*. Cham, Switzerland: Springer Int., Nov. 2021, pp. 118–126.

[43] L. Iafolla, M. Filipozzi, S. Freund, A. Zam, G. Rauter, and P. C. Cattin, "Proof of concept of a novel absolute rotary encoder," *Sens. Actuators A, Phys.*, vol. 312, Sep. 2020, Art. no. 112100.